

Effects of electron-phonon interaction on non-equilibrium transport through single-molecule transistor

Zuo-zi Chen,^{1,*} Rong Lü,¹ and Bang-fen Zhu^{1,2}

¹*Center for Advanced Study, Tsinghua University, Beijing 100084, P. R. China*

²*Department of Physics, and Center for Advanced Study, Tsinghua University, Beijing 100084, P. R. China[†]*

(Dated: December 2, 2024)

The nonequilibrium transport through a single-molecule transistor(SMT) has been investigated with a particular attention paid to the effect of the local electron-phonon interaction and SMT electron-lead coupling on the spectral function and transport properties, in which the Keldysh non-equilibrium Green function technique and canonical transformation method for the local electron-phonon system have been applied. In addition to the usual red-shift, narrowing, and phonon-sidebands of the SMT level due to the electron-phonon interaction, it has been found that, based on the improved decoupling of the electron from phonon system, the profile of the spectral function of the SMT electron is sensitive to lead chemical potentials and can easily be manipulated by tuning the bias as well as the SMT-gate voltage, particularly at zero temperature. Unlike the isolate SMT, the emergence of the phonon sidebands demonstrates the broken electron-hole symmetry in the asymmetric configuration for lead chemical potentials. These electron-phonon interaction effects on the spectral function also manifest themselves in the electronic transport properties.

PACS numbers: 85.65.+h, 73.63.Kv, 73.23.-b, 71.38.-k

I. INTRODUCTION

With the recent progresses in the nanotechnology, it is possible to fabricate and explore the molecular devices.^{1,2} Owing to the promising future of such nano-electronics devices in potential applications and their important roles in understanding the basic physics in the nano-scale, a lot of researches in this area are being carried out, in particular investigating the electrical transport through the single-molecular transistor (SMT), which are sensitive to the local vibration of molecule and exhibit the correlated many-body effect, such as the Coulomb blockade and the Kondo effect.^{3,4,5,6,7}

Theoretically, many efforts have been made to study the quantum transport through the SMT or a quantum dot(QD) by using the kinetic equation approach,⁸ the rate equation approach,⁹ the nonequilibrium quantum theory,^{10,11,12,13} and more recently the numerical renormalization group calculation.¹⁴ In doing such investigations, several groups have already accounted for the electron-phonon interaction(EPI), correlation effects¹⁵, and strong coupling to outside gates.¹⁶

It is well known that the electron-phonon interaction plays a decisive role in transport processes. In the single-molecular transistor, due to strong coupling between the SMT electron and local phonon modes, the EPI should play more important role in the SMT transport. And this may be also true in some quantum dot systems whenever there is strongly coupling between the dot electron and local phonon modes. As an experimental evidence, in a very recent research, Yu *et al.* has reported the inelastic cotunneling features in the SMT transport process.⁷ Meanwhile, since the nano-device is usually connected to the outside gates via the leads, the transport through a SMT or QD is in general a nonequilibrium transport pro-

cess, and a small bias might cause to substantial effect within the nano-scale.

However, there exist contradictory results about the effects of EPI on the transport through the SMT (QD),^{9,10,11,12} because of different approximations used in studying the EPI and decoupling the electron from the phonon system. Although the numerical renormalization group method can well predict the equilibrium properties of the system,¹⁴ it cannot be directly applied to the nonequilibrium case where there is a finite bias voltage. Regarding to the present situation, a theoretical study is certainly required for the nonequilibrium transport of the electron through the SMT or QD, in which strong electron-phonon coupling is taken into proper account.

In this paper we intend to study the effects of a strong local EPI on the quantum transport through the SMT in the presence of finite bias. Unlike the previous investigations, we shall combine the Keldysh nonequilibrium Green function technique with a careful treatment of the decoupling of the electron from the phonon system, based on a nonperturbative canonical transformation for the electron-phonon system. We shall then derive general expressions for the tunneling current and differential conductance, with an emphasis on the joint effects of the EPI and the lead chemical potentials on the SMT electron spectral function. The paper is organized as follows. In section II, an Anderson-Holstein model is presented for the SMT in the presence of local EPI, then our main theoretical framework is described, in which the commonly approximation used in the independent Boson models^{11,18} to decouple the electron from the phonon system is extended. In section III, the numerical results for the spectral function of the SMT electron is demonstrated and discussed, including both the dressing effects due to the EPI and the SMT-leads coupling. An

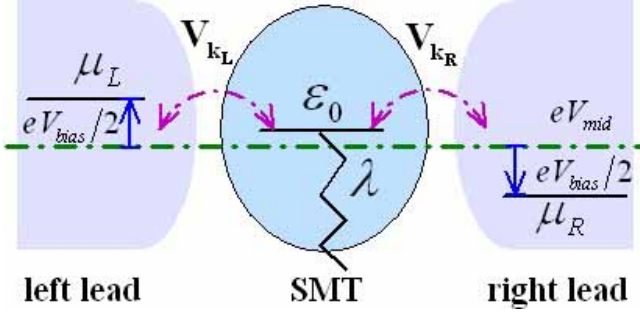


FIG. 1: Schematic illustration for the single-molecule transistor system.

interesting phenomenon is predicted that due to the interplay between the EPI and the molecule-leads coupling, the profile of the spectral function for the SMT electron can be easily manipulated at zero temperature by tuning the chemical potentials in the leads. Consequently, the phonon sidebands in the spectral function may be quite asymmetric with respect to the dressed SMT level, indicating a broken electron-hole symmetry. In section IV, it is shown how the EPI effects on the SMT electron spectral function manifest themselves in the transport properties at both zero temperature and finite temperatures. A special attention is paid to comparing our results with that by using other different decoupling approximations, which might yield nearly the same results at high temperature, but definitely different behaviors at zero temperature. Finally, a brief conclusion is drawn.

II. PHYSICAL MODEL AND FORMALISM

A. Model

As shown in Fig.1, our model for investigation is simply a single electron level in a SMT or QD, which is coupled to the local vibration mode as well as to two leads. For the sake of simplicity, we shall restrict ourselves exclusively to the effect of the EPI and chemical potentials in two leads, thus ignore other factors, such as the intricacies of the real SMT, Coulomb interaction and spin effect. Then the model Hamiltonian can be expressed as

$$\mathbf{H} = \mathbf{H}_{\text{leads}} + \mathbf{H}_{\text{ph}} + \mathbf{H}_{\text{D}} + \mathbf{H}_{\text{T}}, \quad (1)$$

where the first two terms of the Hamiltonian represent the noninteracting electron gas in the leads and the local vibration mode of the SMT, respectively, namely,

$$\mathbf{H}_{\text{leads}} = \sum_{\mathbf{k} \in L(R)} \epsilon_{\mathbf{k}} \mathbf{c}_{\mathbf{k}}^{\dagger} \mathbf{c}_{\mathbf{k}}, \quad \mathbf{H}_{\text{ph}} = \omega_0 \mathbf{a}^{\dagger} \mathbf{a}. \quad (2)$$

Here $\mathbf{c}_{\mathbf{k}}^{\dagger}$ ($\mathbf{c}_{\mathbf{k}}$) creates (annihilates) a conduction electron with momentum \mathbf{k} and energy $\epsilon_{\mathbf{k}}$ in the left (L) or the right (R) lead, ω_0 is the vibrational frequency of the

molecule, and \mathbf{a}^{\dagger} (\mathbf{a}) is the phonon creation (annihilation) operator. The third term \mathbf{H}_{D} describes the coupling between the SMT electron and local phonon mode with strength λ ,

$$\mathbf{H}_{\text{D}} = [\epsilon_0 + \lambda (\mathbf{a} + \mathbf{a}^{\dagger})] \mathbf{d}^{\dagger} \mathbf{d}, \quad (3)$$

where \mathbf{d}^{\dagger} (\mathbf{d}) is the corresponding creation (annihilation) operator of the SMT or QD electron associated with the energy ϵ_0 . The last term \mathbf{H}_{T} describes the hopping of electron between the SMT and leads with the tunneling matrix elements denoted as $V_{\mathbf{k}}$,

$$\mathbf{H}_{\text{T}} = \sum_{\mathbf{k} \in L(R)} [V_{\mathbf{k}} \mathbf{c}_{\mathbf{k}}^{\dagger} \mathbf{d} + \text{h.c.}]. \quad (4)$$

The chemical potentials in the left and right lead are denoted by $\mu_{L(R)}$, respectively, which are related to the bias, V_{bias} , and the average of two lead potentials, V_{mid} , through $V_{\text{bias}} = (\mu_L - \mu_R)/e$ and $V_{\text{mid}} \equiv (\mu_L + \mu_R)/2e$. By changing the external bias and gate voltages experimentally, $\mu_{L(R)}$ and ϵ_0 can be independently adjusted.

Since we are interested in the strong interaction between the SMT electron and local phonon mode, it is appropriate to eliminate the electron-phonon coupling terms in the Hamiltonian by using a nonperturbative canonical transformation, *i.e.*, $\bar{\mathbf{H}} = e^{\mathbf{S}} \mathbf{H} e^{-\mathbf{S}}$ with $\mathbf{S} = \frac{\lambda}{\omega_0} \mathbf{d}^{\dagger} \mathbf{d} (\mathbf{a}^{\dagger} - \mathbf{a})$. The transformed Hamiltonian reads $\bar{\mathbf{H}} = \bar{\mathbf{H}}_{\text{ph}} + \bar{\mathbf{H}}_{\text{el}}$, where the phonon part keeps unchanged, while the electron part is reshaped into

$$\bar{\mathbf{H}}_{\text{el}} = \sum_{\mathbf{k}} \epsilon_{\mathbf{k}} \mathbf{c}_{\mathbf{k}}^{\dagger} \mathbf{c}_{\mathbf{k}} + \tilde{\epsilon}_0 \mathbf{d}^{\dagger} \mathbf{d} + \sum_{\mathbf{k}} [\tilde{V}_{\mathbf{k}} \mathbf{c}_{\mathbf{k}}^{\dagger} \mathbf{d} + \text{h.c.}]. \quad (5)$$

It is clear that due to the EPI, the energy level of SMT is renormalized to $\tilde{\epsilon}_0 \equiv \epsilon_0 - g\omega_0$, where $g \equiv (\lambda/\omega_0)^2$, and the dressed tunneling matrix elements are transformed into $\tilde{V}_{\mathbf{k}} \equiv V_{\mathbf{k}} \mathbf{X}$, where the phonon operator $\mathbf{X} \equiv \exp[-(\lambda/\omega_0)(\mathbf{a}^{\dagger} - \mathbf{a})]$ arises from the canonical transformation of the particle operator $e^{\mathbf{S}} \mathbf{d} e^{-\mathbf{S}} = \mathbf{d} \mathbf{X}$. This reveals that the interaction between the SMT electron and the local phonon mode results in an effective phonon-mediated coupling between the SMT and the lead electrons. When dealing with a localized polaron^{17,18} as in the present case, it is reasonable to replace the operator \mathbf{X} with its expectation value $\langle \mathbf{X} \rangle$, *i.e.*, $\tilde{V}_{\mathbf{k}} = V_{\mathbf{k}} \exp[-g(N_{\text{ph}} + 1/2)]$, where N_{ph} is the phonon population, and can be expressed as $N_{\text{ph}} = 1/[\exp(\beta\omega_0) - 1]$ with $\beta = 1/k_B T$.

B. Formalism

The technique of nonequilibrium Green function developed by Keldysh is one of the most general and successful approaches in dealing with the electronic transport in mesoscopic system^{18,19,20}. By applying it to the present

model, the tunneling current through the SMT can be expressed as^{21,22}

$$J = \frac{ie}{2h} \int d\omega \{ [f_L(\omega) \Gamma^L - f_R(\omega) \Gamma^R] (G^r(\omega) - G^a(\omega)) + (\Gamma^L - \Gamma^R) G^<(\omega) \}, \quad (6)$$

where $f_{L(R)}$ is the Fermi distribution functions in the left (right) lead, $\Gamma^{L(R)}(\epsilon) \equiv 2\pi\rho_{L(R)}(\epsilon) |V_{L(R)}(\epsilon)|^2$, $\rho_{L(R)}(\epsilon)$ is the density of states in the left (right) lead, $V_{L(R)}(\epsilon)$ equals $V_{\mathbf{k} \in L(R)}$ for $\epsilon = \epsilon_{\mathbf{k}}$, and $G^{r(a)}(\omega)$, $G^<(\omega)$ are the Fourier transformations of the standard Keldysh retarded (advanced) and lesser Green functions for the dot electron, respectively.¹⁸ In calculating the current, one needs the spectral function, defined as

$$A(\omega) = i(G^r(\omega) - G^a(\omega)) = i(G^>(\omega) - G^<(\omega)), \quad (7)$$

and the $G^<$ is also proportional to spectral function and the occupation of SMT electron.

When the operator \mathbf{X} is replaced by its expectation value, the Hamiltonian Eq.(5) is decoupled to the phonon operator, then the interacting lesser Green function can be decoupled as

$$\begin{aligned} G^<(t) &\equiv i \langle \mathbf{d}^\dagger(0) \mathbf{d}(t) \rangle = i \langle \bar{\mathbf{d}}^\dagger e^{i\bar{\mathbf{H}}t} \bar{\mathbf{d}} e^{-i\bar{\mathbf{H}}t} \rangle \\ &= i \langle \bar{\mathbf{d}}^\dagger e^{i\bar{\mathbf{H}}_{el}t} \bar{\mathbf{d}} e^{-i\bar{\mathbf{H}}_{el}t} \rangle_{el} \langle \mathbf{X}^\dagger e^{i\bar{\mathbf{H}}_{ph}t} \mathbf{X} e^{-i\bar{\mathbf{H}}_{ph}t} \rangle_{ph} \\ &\equiv \tilde{G}^<(t) e^{-\Phi(-t)}, \end{aligned} \quad (8)$$

and similarly,

$$G^>(t) \equiv -i \langle \mathbf{d}(t) \mathbf{d}^\dagger(0) \rangle = \tilde{G}^>(t) e^{-\Phi(t)}, \quad (9)$$

where $\tilde{G}^{>(<)}(t)$ is the dressed greater (lesser) Green function for a dressed SMT electron governed by $\bar{\mathbf{H}}_{el}$, and the factor $e^{-\Phi(\mp t)}$ arises from the trace of the phonon parts $\langle \mathbf{X}^\dagger(0) \mathbf{X}(t) \rangle_{ph}$ or $\langle \mathbf{X}(t) \mathbf{X}^\dagger(0) \rangle_{ph}$, respectively,¹⁸

$$\Phi(t) = g [N_{ph} (1 - e^{i\omega_0 t}) + (N_{ph} + 1) (1 - e^{-i\omega_0 t})] \quad (10)$$

Note that because $\Phi(-t) \neq \Phi(t)$, the decoupling approximation used in the previous studies,^{11,19} which directly decouples the retarded (advanced) Green function as

$$G^{r(a)}(t) = \tilde{G}^{r(a)}(t) e^{-\Phi(t)}, \quad (11)$$

has ignored the difference between the N_{ph} and $N_{ph} + 1$ in the expression of $\Phi(t)$. Although such approximation works well at high temperature, because $N_{ph} \approx N_{ph} + 1$, it does make difference at low temperature because of vanishing N_{ph} . We shall further discuss this point latter.

By using the identity $e^{-\Phi(t)} = \sum_{n=-\infty}^{\infty} L_n e^{-in\omega_0 t}$, the greater and lesser Green functions can be respectively expanded as

$$\begin{aligned} G^>(\omega) &= \sum_{n=-\infty}^{\infty} L_n \tilde{G}^>(\omega - n\omega_0), \\ G^<(\omega) &= \sum_{n=-\infty}^{\infty} L_n \tilde{G}^<(\omega + n\omega_0), \end{aligned} \quad (12)$$

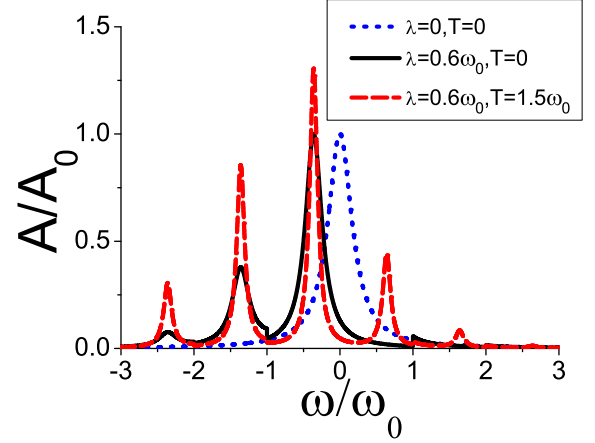


FIG. 2: The dimensionless Spectral function of the SMT electron for different EPI strengths and temperatures. The parameters for calculation are taken as: $\Gamma = 0.2\omega_0$, $\mu_L = \mu_R = \epsilon_0 = 0$, and the unit $A_0 = 2/\Gamma$. The strength of the EPI used here is the same as the references²³.

where the index n stands for the number of phonons involved, and L_n are the coefficients depending on temperature and the strength of EPI. At finite temperature,

$$L_n \equiv e^{-g(2N_{ph}+1)} e^{n\omega_0\beta/2} I_n \left(2g\sqrt{N_{ph}(N_{ph}+1)} \right), \quad (13)$$

where $I_n(z)$ is the n -th Bessel function of complex argument. At zero temperature, L_n simply reads

$$L_n \equiv \begin{cases} e^{-g\frac{g^n}{n!}} & n \geq 0 \\ 0 & n < 0 \end{cases} \quad (14)$$

Thus the spectral function can be expressed as

$$A(\omega) = \sum_{n=-\infty}^{\infty} iL_n [\tilde{G}^>(\omega - n\omega_0) - \tilde{G}^<(\omega + n\omega_0)] \quad (15)$$

With the help of the equation of motion approach, the retarded (advanced) Green function for the dressed electron can be analytically evaluated as

$$\tilde{G}^{r(a)}(\omega) = \frac{1}{\omega - \tilde{\epsilon}_0 - \tilde{\Sigma}^{r(a)}(\omega)}, \quad (16)$$

where the retarded (advanced) self-energy is

$$\tilde{\Sigma}^{r(a)}(\omega) = \sum_{k \in L, R} \frac{|\tilde{V}_k|^2}{\omega - \epsilon_k \pm i\eta} = \tilde{\Lambda}(\omega) \mp i\tilde{\Gamma}(\omega). \quad (17)$$

For simplicity, in the wide-band limit, both the real and the imaginary part of the self-energy, $\tilde{\Lambda}(\omega)$, and $\tilde{\Gamma}(\omega)$, are assumed to be constants independent of energy. Thus, when the self-energy shift is absorbed into the SMT level

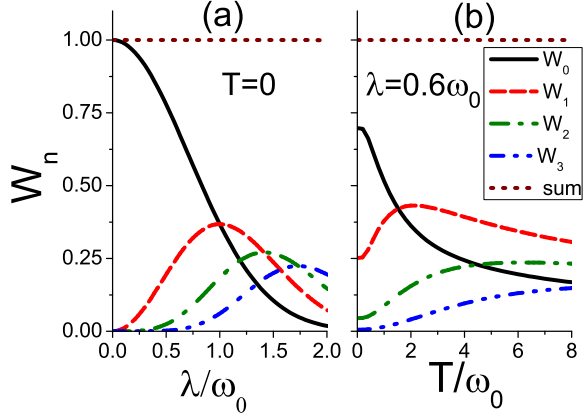


FIG. 3: The total weights of the $+n$ -th and the $-n$ -th phonon sidebands, W_n , as functions of the (a) strength of EPI λ and (b) temperature T , where $\Gamma = 0.2\omega_0$, while $\mu_{L(R)}$ are arbitrary. The dot lines are the numerical summation, $\sum_n W_n$.

renormalization, only the broadening due to the tunnel coupling will be considered. With the assumption of symmetric coupling, $\tilde{\Gamma}^L \approx \tilde{\Gamma}^R = \tilde{\Gamma}$, the broadening can be expressed as $\tilde{\Gamma}(\omega) = (\tilde{\Gamma}^L + \tilde{\Gamma}^R)/2 = \tilde{\Gamma}$. Then the spectral function of the dressed SMT electron can be cast into

$$\tilde{A}(\omega) = \frac{2\tilde{\Gamma}}{(\omega - \tilde{\epsilon}_0)^2 + \tilde{\Gamma}^2}. \quad (18)$$

Following the Keldysh equation²⁰ for the lesser Green function, *i.e.*, $\tilde{G}^<(\omega) = \tilde{G}^r(\omega)\tilde{\Sigma}^<(\omega)\tilde{G}^a(\omega)$ with $\tilde{\Sigma}^<(\omega) = i\tilde{\Gamma}(f_L(\omega) + f_R(\omega))$, the relation between the dressed greater or lesser Green function and the dressed spectral function is respectively as

$$\begin{aligned} \tilde{G}^>(\omega) &= -i \frac{2 - f_L(\omega) - f_R(\omega)}{2} \tilde{A}(\omega), \\ \tilde{G}^<(\omega) &= i \frac{f_L(\omega) + f_R(\omega)}{2} \tilde{A}(\omega). \end{aligned} \quad (19)$$

Thus the spectral function of the SMT electron $A(\omega)$ can readily be obtained by substituting Eqs.(19) and (18) into Eq.(15).

III. THE SPECTRAL FUNCTION OF THE SMT ELECTRON

A. The dressing effects caused by the EPI

The spectral function for our structure generally depends on the EPI strength, temperature, and chemical potential in two leads relative to the SMT level. Let us first focus on the effect of the EPI strength and temperature under the circumstances that $\mu_L = \mu_R = \epsilon_0$.

The spectral functions of the SMT electron are calculated in the presence of the EPI at zero and finite temperature. For comparison, the spectral function without the EPI at 0K is also shown, which exhibits a single resonant peak at ϵ_0 with a Lorentzian lineshape. Compared with the EPI-free case, the spectral function in the presence of finite EPI is red-shifted by $g\omega_0$, and the corresponding phonon-bands are sharpened. This results from the renormalized effects on the SMT level ϵ_0 and the dressing effect on the tunneling matrix elements $V_{\mathbf{k}}$ owing to the EPI. More noticeably, new satellite peaks may appear at $\tilde{\epsilon}_0 \pm n\omega_0$, implying that due to the EPI the ground state for the coupled system may possess finite components involving n phonons. For later convenience, we label the resonant peak located at $\tilde{\epsilon}_0$ as the zero-phonon band, and the satellite peaks located at $\tilde{\epsilon}_0 \pm n\omega_0$ as the $\pm n$ -th phonon sidebands. In general, these phonon sidebands are not symmetric with respect to $\tilde{\epsilon}_0$. By using the identity

$$\begin{aligned} i \int_{-\infty}^{\infty} d\omega (\tilde{G}^>(\omega - n\omega_0) - \tilde{G}^<(\omega + n\omega_0)) \\ = i \int_{-\infty}^{\infty} d\omega (\tilde{G}^>(\omega) - \tilde{G}^<(\omega)) = 2\pi, \end{aligned} \quad (20)$$

and $\sum_{n=-\infty}^{\infty} L_n = \Phi(0) = 1$, it can be easily examined that the sum rule for the spectral function still holds in the presence of EPI, namely

$$\int_{-\infty}^{\infty} d\omega A(\omega) = 2\pi. \quad (21)$$

As shown in Fig.2, the weight of each peak, defined as the integrated area under the peak divided by 2π and denoted by $W_{\pm n}$, is sensitive to the EPI strength and temperature. We can further define summation of the spectral weights of the $+n$ -th and $-n$ -th phonon sidebands as

$$\begin{aligned} W_n \equiv W_{+n} + W_{-n} = L_n + L_{-n} = e^{-g(2N_{ph}+1)} \\ \times (e^{n\omega_0\beta/2} + e^{-n\omega_0\beta/2}) I_n \left(2g\sqrt{N_{ph}(N_{ph}+1)} \right) \end{aligned} \quad (22)$$

Fig.3 shows that when λ or T increases, the spectral weight of the zero-phonon band, W_0 decreases monotonically; while the phonon sideband, W_n ($n \neq 0$), gets larger up to certain value of the temperature or EPI strength, then decreases again, one by one. This reflects when increasing the temperature or EPI strength, the occupation probability of the phonon sideband increases, keeping the conservation of the total spectral weight, *i.e.*, $\sum_{n=0}^{\infty} W_n = 1$.

B. The interplay between the EPI and the SMT electron-lead coupling

Now let us take a close look at the dependence of the spectral function of the SMT electron on the chemical potentials in two leads in the presence of the EPI.

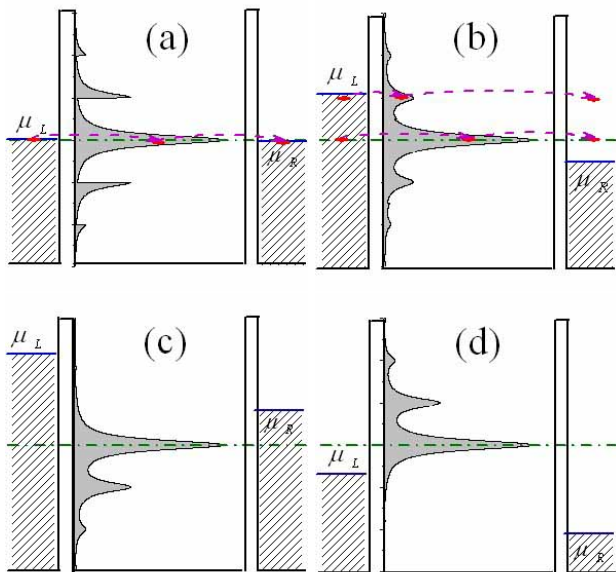


FIG. 4: The spectral functions of the SMT electron for four typical configurations of $\mu_{L(R)}$: (a) $\mu_L = \mu_R = \tilde{\epsilon}_0$, (b) $\mu_L = \tilde{\epsilon}_0 + 0.9\omega_0$, $\mu_R = \tilde{\epsilon}_0 - 0.5\omega_0$, (c) $\mu_L = \tilde{\epsilon}_0 + 2.2\omega_0$, $\mu_R = \tilde{\epsilon}_0 + 0.8\omega_0$, (d) $\mu_L = \tilde{\epsilon}_0 - 0.8\omega_0$, $\mu_R = \tilde{\epsilon}_0 - 2.2\omega_0$, where the parameters are $\Gamma = 0.2\omega_0$, $\lambda = 0.6\omega_0$, $T = 0$ and $\tilde{\epsilon}_0 = 0$. The balls connected by the dash lines in (a) and (b) denote the resonant tunneling processes for electrons.

As shown in Fig.4, it is quite interesting that the spectral function of the SMT electron profiles quite differently for the same EPI strength and temperature ($0K$), but under different configurations of the chemical potentials in two leads. And the phonon sidebands, whose lineshapes may vary abruptly at certain frequency, can be nonvanishing in both sides of the zero-phonon band, even at zero temperature. This is quite different from the Independent Boson model, according to which, the phonon sidebands have nothing to do with the lead chemical potentials, and at zero temperature, they should vanish on the negative energy side of the zero-phonon band.

The unusual behavior of the present spectral function can be understood with Eqs.(15) and (19), in which the expansion $\tilde{G}^>(\omega - n\omega_0)$, and $\tilde{G}^<(\omega + n\omega_0)$ in general depends on the Fermi function of $f_L(f_R)$ in the left (right) lead, and thus on the chemical potential, $\mu_L(\mu_R)$, respectively. At zero temperature, the coefficients L_n vanish for negative n , therefore only to the zero-phonon band of the spectral function both the lesser and greater Green function make contribution; while the phonon sidebands below the zero-phonon band result from the $\tilde{G}^<(\omega + n\omega_0)$, and those above the zero-phonon band come from the $\tilde{G}^>(\omega - n\omega_0)$.

Recalling that the lesser and greater Green functions $\tilde{G}^{<(>)}$ correspond to the dressed SMT electron and hole propagator, which are proportional to the occupation number of the SMT electron, n_{SMT} , or hole, $1 - n_{SMT}$

respectively. In the present system, n_{SMT} is determined by the Fermi distributions in both leads. Compared to the Independent Boson Model, where n_{SMT} is assumed to be fixed to be zero or one, n_{SMT} here can vary from zero to one. In this case, the contribution from both the SMT electron and hole to the spectral function should not be neglected. It is just the different treatment of n_{SMT} that leads to the unusual behavior of the phonon sidebands at low temperature. At zero temperature, no phonon is available, the SMT electron and hole can only emit phonons. Thus the phonon sidebands below the zero-phonon band come from the occupative SMT electron, while those above the zero-phonon band originate from the SMT hole. Therefore, if there is a partial occupation in the zero-phonon band for the SMT electron, it is necessary at low temperature to carefully examine the contribution from both electron and hole.

The spectral function can be explicitly expressed as functions of the bias and V_{mid} , the average of two lead potentials relative to the renormalized SMT level as defined in the Section II, *i.e.*, $A(\omega, V_{mid}, V_{bias})$. In this way the effect due to the bias and due to the V_{mid} on the spectral function will be considered separately. We have found that the V_{mid} mostly affects the lineshape of the spectral function in the present model. Four typical configurations of the lead chemical potentials in Fig.4 are divided into two categories: (1) The $V_{mid} \sim \tilde{\epsilon}_0$, when the SMT level is nearly half filled, *i.e.* $n_{SMT} \sim 0.5$. Then for either bias in Fig.4(a) or Fig.4(b), the resonant tunneling can take place. (2) The V_{mid} deviates from $\tilde{\epsilon}_0$ significantly compared with the band-width $\tilde{\Gamma}$, so that the SMT level is either fully occupied or totally empty, *i.e.* $n_{SMT} \simeq 1$ (Fig.4(c)), or $n_{SMT} \simeq 0$ (Fig.4(d)), in which no resonant tunneling can occur.

In Fig.4(a), both chemical potentials in the leads align exactly with the renormalized SMT level, where the lineshape of each phonon sideband exhibits discontinuity at certain frequency. This is similar to the case $\mu_L = \mu_R = \epsilon_0$ (*cf.* Fig.2), except for that the spectral function is symmetric with respect to $\tilde{\epsilon}_0$, while asymmetric for the case of $\mu_L = \mu_R = \epsilon_0$. It is reasonable, because at zero bias and zero temperature there exist a well-defined boundary, $\mu_L = \mu_R$, dividing the SMT electron from hole. The symmetric spectral function is solely an exception when the renormalized SMT level happens to coincide with the boundary. In Fig.4(b), when the bias is large enough to enclose the most part of the zero-phonon band, both distributions of the SMT electron or hole in the zero-phonon band become Lorentzian, and so does the lineshape of each phonon sideband. Note that whenever one of the phonon sidebands enters the bias region, there will exist the phonon-assisted tunneling process. Compare Fig.4(b) to (a), it is evident that the bias is not only important in determining the profile of each phonon sideband, but also crucial in controlling of the phonon-assisted tunneling. It is interesting to observe that when $n_{SMT} \simeq 0$ (Fig.4(d)), which corresponds to the one-hole picture, the usual result following the Inde-

pendent Boson Model¹⁸ is recovered; on the other hand when $n_{SMT} \simeq 1$ in Fig.4(c), which corresponds to the picture of one-electron, the spectral function is reversed with respect to $\tilde{\epsilon}_0$ compared to (d). Comparison among the four configurations shows that the V_{mid} relative to $\tilde{\epsilon}_0$ has played a decisive role in determining the partition between the SMT electron and hole.

The spectral function has been found to have the symmetry as follows,

$$A(\omega, V_{mid}, -V_{bias}) = A(\omega, V_{mid}, V_{bias}), \quad (23)$$

and

$$\begin{aligned} A(\omega = \tilde{\epsilon}_0 - \Delta\omega, V_{mid} = \tilde{\epsilon}_0/e - \Delta V, V_{bias}) \\ = A(\omega = \tilde{\epsilon}_0 + \Delta\omega, V_{mid} = \tilde{\epsilon}_0/e + \Delta V, V_{bias}). \end{aligned} \quad (24)$$

Compared to the EPI-free case, the spectral function in the EPI is generally asymmetric with respect to $\tilde{\epsilon}_0$ unless $eV_{mid} = \tilde{\epsilon}_0$. This implies a broken electron-hole symmetry, which can also be seen from Fig.4, where the spectral functions in both (a) and (b) are symmetric with respect to $\tilde{\epsilon}_0$; while in Fig.4(c) and (d), there are broken symmetry for electron and hole obviously.

With increasing temperature, one can expect that the profile of the dot spectral function should be less and less sensitive to the variation of the lead chemical potentials, because the Fermi distribution varies continuously across $\mu_{L(R)}$ at high temperature, so does the phonon sidebands.

IV. THE TRANSPORT PROPERTIES

Based on the spectral function discussed above, in this section, we shall investigate the differential conductance and tunneling current of the SMT(QD) system. The case of zero temperature will be discussed first, then follows the modifications from the finite temperature effect.

A. The zero temperature

At zero temperature, the Fermi distribution functions are the step functions $\Theta(\mu_{L(R)} - \omega)$, and the coefficients L_n reduce to the Eq.14, thus the current can be expressed explicitly as

$$\begin{aligned} J = \frac{e}{4h} \sum_{n=0}^{\infty} L_n \Gamma \int d\omega [\Theta(\mu_L - \omega) - \Theta(\mu_R - \omega)] \left\{ [\Theta(\mu_L - \omega - n\omega_0) + \Theta(\mu_R - \omega - n\omega_0)] \tilde{A}(\omega + n\omega_0) \right. \\ \left. + [2 - \Theta(\mu_L - \omega + n\omega_0) - \Theta(\mu_R - \omega + n\omega_0)] \tilde{A}(\omega - n\omega_0) \right\}. \end{aligned} \quad (25)$$

Using $\mu_{L(R)} = eV_{mid} \pm eV_{bias}/2$, and $\partial\Theta(\mu_{L(R)} - \omega)/\partial V_{bias} = \pm e\delta(\mu_{L(R)} - \omega)/2$, the differential conduc-

tance can be obtained by performing $\partial J/\partial V_{bias}$,

$$\begin{aligned} G(V_{mid}, V_{bias}) = \frac{e^2}{8h} \sum_{n=0}^{\infty} L_n \Gamma \left\{ \Theta(eV_{bias} - n\omega_0) [\tilde{A}(\mu_L) + \tilde{A}(\mu_R) + \tilde{A}(\mu_L - n\omega_0) + \tilde{A}(\mu_R + n\omega_0)] \right. \\ \left. + \Theta(-eV_{bias} - n\omega_0) [\tilde{A}(\mu_L) + \tilde{A}(\mu_R) + \tilde{A}(\mu_L + n\omega_0) + \tilde{A}(\mu_R - n\omega_0)] \right\}. \end{aligned} \quad (26)$$

It is easy to verify that the tunneling current and differential conductance satisfy the symmetry relations as

$$\begin{aligned} J(V_{mid} = \tilde{\epsilon}_0/e - \Delta V, V_{bias}) = J(V_{mid} = \tilde{\epsilon}_0/e + \Delta V, V_{bias}), \\ G(V_{mid} = \tilde{\epsilon}_0/e - \Delta V, V_{bias}) = G(V_{mid} = \tilde{\epsilon}_0/e + \Delta V, V_{bias}), \end{aligned}$$

and

$$\begin{aligned} J(V_{mid}, -V_{bias}) &= -J(V_{mid}, V_{bias}), \\ G(V_{mid}, -V_{bias}) &= G(V_{mid}, V_{bias}). \end{aligned} \quad (27)$$

Note that due to the equivalence between the current of electron type and hole type, the broken symmetry with respect to $\tilde{\epsilon}_0$ in the spectral function of SMT electron is now restored for the tunneling current and differential conductance.

The map plotted in Fig.5 is the calculated differential conductance as functions of V_{mid} and V_{bias} in the presence of the EPI. The dashed lines in Fig.5(a) and (b) represent the differential conductance for a fixed value of $eV_{bias}^{fix} = 3.6\omega_0$ and $eV_{mid}^{fix} = 0.8\omega_0$, respectively; while

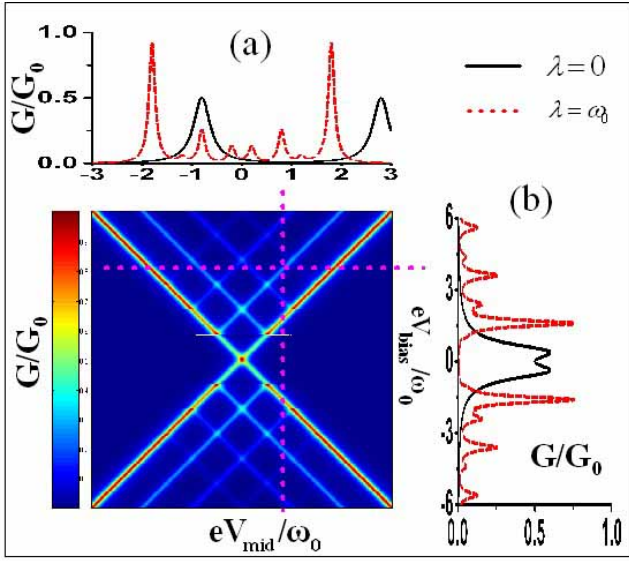


FIG. 5: (Color on line) The dimensionless differential conductance ($G_0 = e^2/2h$) at $T = 0K$ as functions of V_{mid} and V_{bias} . The parameters for calculation are taken as: $\Gamma = 0.2\omega_0$, $\epsilon_0 = \omega_0$, and $\tilde{\epsilon}_0 = 0$ which implies that for the sake of clarity a stronger EPI strength, $\lambda = \omega_0$, is chosen. The color scale runs from zero (blue) to G_0 (red). The above (a) and right (b) panel to the map are the sections for a fixed value of $eV_{bias}^{fix} = 3.6\omega_0$ and $eV_{mid}^{fix} = 0.8\omega_0$, respectively, marked on the map with dash lines.

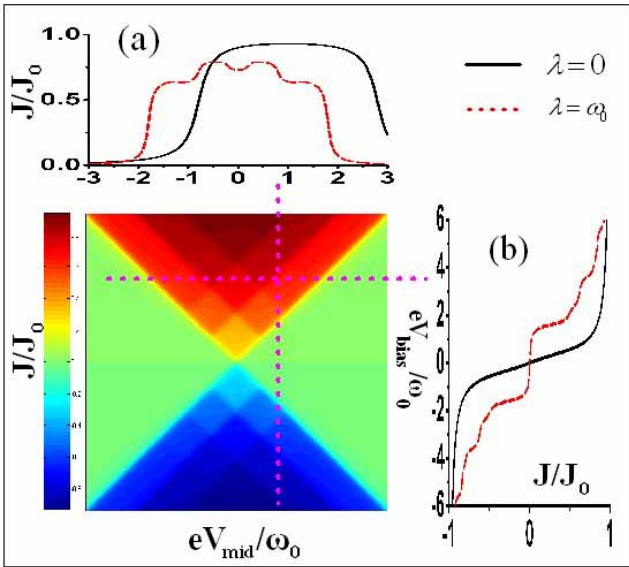


FIG. 6: (Color on line) The map of tunneling current, $J(V_{mid}, V_{bias})$, at $T = 0K$, where the parameters are taken as the same as the Fig.5, and $J_0 = e\Gamma/2\hbar$. The color scale runs from $-0.9J_0$ (blue) to $0.9J_0$ (red). The solid and dashed lines in sections (a) and (b) represent the tunneling current for the cases without and with EPI, respectively.

the solid lines correspond to the differential conductance without the EPI as for reference, in which the peaks appear only when one of the lead chemical potentials is aligned with the SMT level, *i.e.*, $\mu_L(\mu_R) = \epsilon_0$. Compared with the EPI-free case, the corresponding peaks in the presence of finite EPI are sharpened, and red-shifted by $g\omega_0$, and more noticeably, new satellite peaks are shown up, which are associated with the phonon-assisted tunneling processes as depicted in Fig.4(b), when $\mu_L = \tilde{\epsilon}_0 + n\omega_0$ or $\mu_R = \tilde{\epsilon}_0 - n\omega_0$ for $V_{bias} \geq 0$; $\mu_L = \tilde{\epsilon}_0 - n\omega_0$ or $\mu_R = \tilde{\epsilon}_0 + n\omega_0$ for $V_{bias} < 0$, where $n \leq \Theta(|eV_{bias}|/\omega_0)$.

The map plotted in Fig.6 is the tunneling current as functions of V_{mid} and V_{bias} , which can be divided into several plateaus with the bounded lines corresponding to the differential conductance peaks in Fig.5. It should be pointed out that the phonon-assisted tunneling can take place even at zero temperature. Although no thermal phonon is available at $0K$, the phonon-emitted process accompanying the tunnel is possible, if the phonon energy can be supplied by the bias voltage across the SMT. As also shown in the map (Fig.5), the phonon-assisted peaks are absent in the left and right quarters, which are bounded by the lines of the zero-phonon peaks.

Now let us take a look at the relationship between the transport properties and the SMT spectral function. As discussed above, due to the dressing effects of EPI, the SMT electron still has finite probabilities to occupy the phonon sidebands even at zero temperature. Once the phonon sideband of the SMT enters the bias region, the phonon-assistant-channel would be open, as depicted in Fig.4(b). Thus the information of the SMT spectral function can be inferred from the spectra of the tunneling current or differential conductance. For example, for a fixed V_{mid} , the integral of the differential conductance over V_{bias} satisfies a sum rule, $\int_{-\infty}^{\infty} dV_{bias} G(V_{mid}, V_{bias}) = J_0$, which just results from the conservation of the spectral weights in Eq.(21). While for a fixed V_{bias} , the integral of the differential conductance over V_{mid} does not equal J_0 in consequence of the transfer of a finite spectral weights to those phonon sidebands, which do not participate in tunneling. This is a little different from the tunneling process without the EPI, where the sum rule for the differential conductance always holds.

We will end this subsection with a comparison between the results based on different decoupling approximations, *i.e.*, Eq.(9) and Eq.(11). In the zero bias limit, by taking Eq.(9) as we have done, the differential conductance would have no phonon-assisted peaks as clearly shown in Fig.5. On the other hand, by following Eq.(11), there would be a set of non-vanishing phonon-assisted peaks in the differential conductance^{10,11,18,19,21}. This discrepancy can be explained in terms of the different SMT spectral functions obtained in different approximations. Once the Green function is decoupled according to Eq.(11), the SMT spectral function would be expanded in the follow-

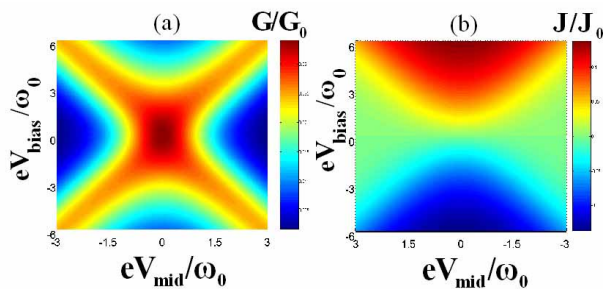


FIG. 7: (Color on line) The dimensionless differential conductance and tunneling current as functions of V_{mid} and V_{bias} , (a) $G(V_{mid}, V_{bias})$, (b) $J(V_{mid}, V_{bias})$, where $\Gamma = 0.2\omega_0$, $\lambda = \omega_0$, $T = 0.6\omega_0$, $\tilde{\epsilon}_0 = 0$, and the units $G_0 = e^2/2h$, $J_0 = e\Gamma/2\hbar$. The color scale runs from zero conductance (blue) to $0.05G_0$ (red) in (a) and from $-0.15J_0$ (blue) to $0.15J_0$ (red) in (b).

ing way,

$$B(\omega) = \sum_{n=-\infty}^{\infty} L_n \left[\tilde{A}(\omega - n\omega_0) \right]. \quad (28)$$

At zero temperature, we have $n \geq 0$, the profile of $B(\omega)$ is similar to Fig.4(d), namely there is a set of non-vanishing

$$F_n(\omega) = \frac{\beta}{2} \left\{ [f_L(\omega)(1 - f_L(\omega)) + f_R(\omega)(1 - f_R(\omega))] \left[1 + \frac{e^{-\beta n\omega_0} - 1}{2} (f_L(\omega - n\omega_0) + f_R(\omega - n\omega_0)) \right] \right. \\ \left. + \frac{e^{-\beta n\omega_0} - 1}{2} (f_L(\omega) - f_R(\omega)) [f_L(\omega - n\omega_0)(1 - f_L(\omega - n\omega_0)) - f_R(\omega - n\omega_0)(1 - f_R(\omega - n\omega_0))] \right\}. \quad (30)$$

Both maps for the differential conductance and tunneling current at finite temperature are plotted in Fig.7. Compared to the zero temperature case, the differential conductance peaks at finite temperature are broadened and smeared out to some extent, and the tunneling current profile become smoother and less sensitive to the bias, which results from the smoother Fermi distributions in the leads at finite temperature. Note also that, since the phonon sidebands of the spectral function will distribute more symmetrically around the zero-phonon-peak at finite temperature than the $0K$ case as shown in Fig.2, the phonon-assisted peaks of the differential conductance might appear in the two forbidden quarters as shown in Fig.5 at $0K$. Therefore, the difference caused by the different decoupling approximations as discussed above will be diminished with increasing the temperatures.

phonon sidebands above the zero-phonon band, which is independent of the Fermi distributions in the leads. Thus, following the approximation (11), in the zero bias limit, the differential conductance would exhibit a set of phonon peaks. Physically, our results which follow Eqs. (9) and (8), seem more reasonable, because the tunneling electron can neither absorb nor emit any phonon in the zero temperature and zero bias limit.

B. finite temperature

The tunneling current at finite temperature can readily be obtained from Eq.(6). With the help of the identities $L_{-n} = e^{-\beta n\omega_0} L_n$ and $\partial f_{L(R)}(\omega)/\partial V_{bias} = \pm e\beta f_{L(R)}(\omega)(1 - f_{L(R)}(\omega))/2$, the differential conductance can be expressed in a compact form:

$$G = \frac{e^2\Gamma}{2h} \sum_{n=-\infty}^{\infty} L_n \int_{-\infty}^{\infty} d\omega F_n(\omega) \tilde{A}(\omega - n\omega_0), \quad (29)$$

where the factors $F_n(\omega)$ depend on the Fermi distributions in the leads through,

V. CONCLUSION

In summary, we have theoretically studied the non-equilibrium quantum transport through the single molecule transistor or quantum dot in the presence of the local electron-phonon interaction. Owing to the EPI, the spectral function of the dot electron will manifest itself in the phonon-dressing effects, such as the red-shift and narrowing of the zero phonon peak, and the transfer of finite spectral weights to the phonon sidebands. Furthermore, due to the interplay between the EPI and the dot-lead coupling, the phonon sidebands of the dot electron spectral function at $0K$ can easily be manipulated. Namely, although the sum of the spectral weights for the $+n$ -th and $-n$ -th phonon sideband is fixed for a given temperature and EPI strength, the distribution of the spectral weights is critically dependent on the chemical potentials in two leads, in particular on the average of two lead potentials relative to the renormalized SMT level, showing the broken electron-hole symmetry. The tunneling current and differential conductance have been analyzed at

both zero and finite temperatures, which also reveal the dependence on the chemical potentials of the leads. Different approximations used in decoupling the electron-phonon system have been compared and discussed in the zero bias limit. It has been found that although different decoupling approximations can yield nearly the same results at high temperature, they do lead to quite different behaviors at zero temperature.

Acknowledgement: The authors would like to thank H. Zhai, H. Z. Lu and C. X. Liu for useful discussions. This work is supported by the Natural Science Foundation of China (Grant No. 90103027, 10374056), the MOE of China (Grant No.200221, 2002003089), and the Program of Basic Research Development of China (Grant No. 2001CB610508).

-
- * Electronic address: zzchen@castu.tsinghua.edu.cn
 † Electronic address: bfzhu@castu.tsinghua.edu.cn
- ¹ H. Park, et al., Nature **407**, 57 (2000).
 - ² J. Reichert, et al., Phys. Rev. Lett. **88**, 176804 (2002).
 - ³ J. Park, et al., Nature **417**, 722 (2002).
 - ⁴ S. Kubatkin, et al., Nature **425**, 698 (2003).
 - ⁵ W. Liang, et al., Nature **417**, 725 (2002).
 - ⁶ H. Y. Lam and D. Natelson, cond-mat/0405568.
 - ⁷ L. H. Yu, et al., cond-mat/0408052 v1.
 - ⁸ D. Boese and H. Schoeller, Europhys. Lett. **54**, 668 (2001); K. D. McCarthy, N. Prokof'ev, and M. T. Tuominen, cond-mat/0205419.
 - ⁹ A. Mitra, I. Aleiner, A. J. Millis, Phys. Rev. B **69**, 245302 (2004).
 - ¹⁰ U. Lundin and R. H. McKenzie, Phys. Rev. B **66**, 075303 (2002).
 - ¹¹ J.-X. Zhu and A. V. Balatsky, Phys. Rev. B **67**, 165326 (2003).
 - ¹² N. S. Wingreen, K. W. Jacobsen, and J. W. Wilkins, Phys. Rev. B **40**, 11834 (1989).
 - ¹³ A. O. Gogolin and A. Komnik, cond-mat/0207513.
 - ¹⁴ P. S. Cornaglia, H. Ness, and D. R. Grempel, Phys. Rev. L **93**, 147201 (2004).
 - ¹⁵ A. S. Alexandrov and A. M. Bratkovsky, Phys. Rev. B **67**, 235612 (2003).
 - ¹⁶ K. Flensberg, Phys. Rev. B **68**, 205323 (2003); Phys. Rev. B **68**, 205324 (2003).
 - ¹⁷ A. Hewson and D. Newns, J. Phys. C **13**, 4477 (1980).
 - ¹⁸ G. D. Mahan, *Many-Particle Physics*, 3rd ed. (Plenum Press, New York, 2000).
 - ¹⁹ H. Huag and A. -P. Jauho in *Quantum Kinetics in Transport and Optics of Semiconductors*, edited by Dr. -Ing. Helmut K. V. Lotsch (Springer-Verlag, Berlin Heidelberg, 1996).
 - ²⁰ D. C. Langreth, in *Linear and Nonlinear Electron Transport in Solids*, edited by J. T. Devreese and V. E. Van Doren (Plenum, New York, 1976).
 - ²¹ A. -P. Jauho, N. S. Wingreen and Y. Meir, Phys. Rev. B. **50**, 5528 (1994).
 - ²² Y. Meir and N. S. Wingreen, Phys. Rev. Lett. **68**, 2512 (1992).
 - ²³ M.-T. Kuo David and Y. C. Chand, Phys. Rev. B **66**, 085311 (2002).